Biosensors and Bioelectronics 51 (2014) 274–279

Contents lists available at ScienceDirect

Biosensors and Bioelectronics

journal homepage: www.elsevier.com/locate/bios

Short communication

Whole-cell *Escherichia coli*-based bio-sensor assay for dual zinc oxide nanoparticle toxicity mechanisms

Jonathan S. Mcquillan, Andrew M. Shaw*

Biosciences, College of Life and Environmental Sciences, University of Exeter, Exeter EX4 4QD, UK

ARTICLE INFO

Article history:
Received 8 April 2013
Received in revised form
13 June 2013
Accepted 12 July 2013
Available online 22 July 2013

Keywords:
Zinc oxide nanoparticle
Escherichia coli
Stress response
Whole cell biosensor
Real time PCR

ABSTRACT

A whole-cell biosensor assay for dual ZnO nanoparticle toxicity mechanisms has been developed based on the transcriptional response of *Escherichia coli* to: (1) Zn^{2+} from ZnO nanoparticle dissolution with genes *zntA* (Zn^{2+} efflux) and *znuABC* (Zn^{2+} uptake); and (2) redox stress from ZnO nanoparticle photo-electron production under ultraviolet light with genes *soxS* and *katG*. Both processes occur in a dispersion of ZnO nanoparticles leading to toxicity. ZnO nanoparticle dissolution was measured independently by ICP-MS and photo-radical generation was confirmed by the stochiometric reduction of the redox dye, 2, 6-dichloroindolphenol (DCPIP). The whole-cell biosensor can detect both toxicity mechanisms and is a species-specific assay capable of discriminating between ZnO nanoparticles and the Zn^{2+} dissolution product.

1. Introduction

Zinc oxide nanoparticles are produced in high tonnage industrially for incorporation into a number of products including sunscreen and cosmetics, ultimately ending up in the environment with potential toxicological effects (Klingshirn, 2007). The direct mechanism for ZnO nanoparticle toxicity is dissolution and release of zinc ions (Gulson et al., 2010; Miao et al., 2010). A second toxicity mechanism is the generation of photo-radicals by ZnO nanoparticles in ultraviolet light, promoting electrons across the material band gap (Comparelli et al., 2005; Hoffmann et al., 1995; Mills and Le Hunte, 1997). The two toxicity mechanisms together offer a species-specific assay for ZnO nanoparticles in complex media. Both mechanisms can be ameliorated by the presence of surface ligands (Mitchnick et al., 1999; Waalewijn-Kool et al., 2013) but the efficacy of the ligand-induced reduction in toxicity requires a reliable, quality assured assay. However, both toxicity mechanisms are difficult to measure physically in the environment or complex media where zinc ions are quickly dispersed and free radicals are rapidly neutralised with half-lives in the order of nanoseconds.

Whole cell biosensors offer an alternative approach to physical methods for detecting toxic substances (Bousse, 1996), specifically where transcriptional biomarkers for a toxic stress response are measured minutes-hours following exposure. These typically feature promoter-reporter gene fusion constructs whereby positive regulation of the gene corresponds to an increase in a detectable product (Mitchell and Gu, 2004; Riether et al., 2001). Specifically, recombinant reporter strains of *E. coli* have been used to probe Zn^{2+} toxicity (Ivask et al., 2010; Ivask et al., 2002, 2009). However, an alternative approach is to detect changes in gene regulation directly in non-recombinant strains by measuring levels of the corresponding gene transcript by real-time PCR. This allows simultaneous measurement of two toxicity mechanisms using multiple transcriptional biomarkers for the corresponding stress responses as it does not require individual promoter-reporter constructs for each gene.

E. coli bacteria are particularly suited as whole-cell biosensors as the role of individual genes and proteins has been intensively studied (Keseler et al., 2011). Specifically, the organism responds to excess Zn^{2+} by regulating the expression of genes encoding divalent cation-specific transporters that control the flux of Zn^{2+} across the plasma membrane (Yamamoto and Ishihama, 2005). Specifically, ZnuABC is a Zn^{2+} import protein (Patzer and Hantke, 1998), which is regulated through the activity of the Zinc Uptake Regulator (Zur) (Patzer and Hantke, 2000), and ZntA is a Zn^{2+} efflux protein (Beard et al., 1997; Binet and Poole, 2000; Rensing et al., 1997) which is regulated through the activity of ZntR (Brocklehurst et al., 1999; Outten et al., 1999). The genes are inversely regulated in response to femtomolar changes in the free Zn^{2+} concentration in the cytosol (Outten and O'Halloran, 2001). Similarly, the *E. coli* SoxR and OxyR proteins are redox-dependant switches that regulate the expression of genes to counteract oxidative stress (Demple, 1999). SoxR is activated by oxidation of redox-sensitive Fe–S clusters and promotes transcription of a

* Corresponding author. Tel.: +44 1392263495; fax: +44 1392263434.
E-mail address: andrew.m.shaw@exeter.ac.uk (A.M. Shaw).

0956-5663/$ - see front matter © 2013 Elsevier B.V. All rights reserved.
http://dx.doi.org/10.1016/j.bios.2013.07.024

second transcription factor, SoxS which regulates multiple anti-oxidant functions including expression of superoxide dismutase genes *sodA* and *sodC*. OxyR is activated by oxidation of cysteine residues and di-sulfide bond formation leading to gene regulatory activity including the positive regulation of *katG*, a gene encoding Catalase; a potent antioxidant.

In this study, we use the *E. coli* bacterium as a whole cell biosensor for simultaneous detection of the ZnO nanoparticle toxicity mechanisms. We show physically the dissolution of ZnO nanoparticles in a complex medium supporting bacterial growth (Neidhardt's medium (Neidhardt et al., 1974)) using ultra-centrifugation and total Zn determination by ICP-MS, and also the rate of photo-electron production leading to a stoichiometric colour change in the redox dye DCPIP. Both dissolution and photo-radical generation are toxic to the bacterium and activate changes in gene transcription which can be utilised as biomarkers for both toxicity mechanisms in a single assay.

2. Experimental

2.1. Nanoparticle characterisation and handling

Zinc oxide nanoparticles (Z-COTE®) were purchased from BASF UK (Cheadle, UK). The specific material batch has been characterised by the National Physics Laboratory of the UK (NPL) as part of the Nanotechnology Industries Association (NIA) PROSPECT project (Ecotoxicology Test Protocols for Representative Nanomaterials in Support of the OECD Sponsorship Programme). The dry nanoparticles had a surface area determined by BET isotherm of 12–14 $m^2\ g^{-1}$ and a mean diameter of 150 ± 60 nm, measured by high resolution Scanning Electron Microscopy (SEM) and Transmission Electron Microscopy (TEM).

Experiments were carried out using dispersions of the nanoparticles in water or Neidhardt's medium (Neidhardt et al., 1974). The composition of the medium and details of the dispersion procedure are given in the Supporting information. For TEM analysis the particles were first dispersed in Neidhardt's medium and then the suspension was centrifuged in a vessel containing a polyethylene plug in the bottom supporting copper–palladium 200 mesh grids with carbon-formvar supports (TAAB, Aldermaston, UK). We found that this process coats the grids evenly and reduces drying artefacts. The grids were dried at room temperature before imaging. The nanoparticles were also imaged after suspension with *E. coli* bacteria (MG1655) wherein the samples were fixed in 3% glutaraldehyde in 0.1 M phosphate buffer (pH 7.2) before drying and imaging.

The stability of nanoparticle suspensions was determined by recording absorption spectra using a scanning UV–vis spectrophotometer (Bibby Scientific, Stone, UK) over a time course, wherein a characteristic λ_{max} at 375 nm is indicative of a colloidal suspension.

2.2. Dissolution rate measurements

Zinc oxide nanoparticles were suspended Neidhardt's medium and samples were removed over the time course 0, 1, 2, 5, 11, 23 and 47 h. The nanoparticles were separated from the medium by ultracentrifugation (50,000*g*, 30 min, Beckman) and then the medium was acidified (10% nitric acid) and microwave digested at 200 °C for 10 min (Milestone Inc., Connecticut, USE). Digests were measured with a 7500 ICP-MS (Agilent, UK) in standard analysis mode and total Zn concentration in the samples was determined by measuring the isotopes ^{64}Zn, ^{66}Zn, ^{67}Zn and ^{68}Zn. Quantification was performed by external calibration using Zn standard solutions and ^{103}Rh as an internal standard, correcting each sample for a procedural blank.

2.3. Zinc ion toxicity tests

E. coli K12 (MG1655) were cultured aerobically at 37 °C in Neidhardt's medium with 0.1% (w/v) glucose. Log phase cultures were mixed 1:1 with sterile, pre-warmed minimal salts medium containing zinc oxide nanoparticles or zinc chloride. Viable cell numbers were determined over a time course of 6 h by the plate counting method.

2.4. DCPIP assay for photo-electron production

A suspension of ZnO nanoparticles in deionised water was mixed with an aqueous solution of DCPIP (Sigma, Gillingham, UK) to a final concentration of 1 mM. The mixture was either kept in the dark or irradiated with 375 ± 5 nm light from a lid-mounted LED (NICHIA, Japan) producing a power of 2 mW. Photo-electron production from the ZnO nanoparticles was measured by monitoring the absorbance change at 595 nm using a spectrophotometer. A further $ZnCl_2$ photo-control was also performed: no photo-radicals were detected by the DCPIP assay.

2.5. Photo-electron toxicity tests

Exponentially replicating *E. coli* were harvested by centrifugation (5000*g*, 5 min) and re-suspended with a suspension of the ZnO nanoparticles in deionised water at a density of 10^6 CFU mL^{-1}. The suspensions were irradiated with 375 nm light from the lid-mounted LED used in the DCPIP assay or kept in the dark. Bacterial survival was measured by CFUs compared to the appropriate control; either *E. coli* in water in the dark or *E. coli* in water with 375 nm light.

2.6. Real-time PCR

E. coli cultures were exposed to Zn as described for the zinc ion toxicity tests and exposed to the nanoparticles either in the dark or irradiated with UV radiation at 375 nm. An additional control was exposure to UV without the nanoparticles. The exposure time was 10 min. The abundance of specific mRNA sequences in the total RNA extracted from the suspensions was compared to untreated controls, which were *E. coli* in unmodified minimal salts medium in the dark. Real time PCR was carried out using the SYBR green DNA detection chemistry and the method of Pfaffl (Pfaffl, 2001), and as described in other work (McQuillan et al., 2012). Primer sequences are listed in the Supporting information, Table S1. The internal reference gene was *rrsB* as used by others in metal stress measurements for *E. coli* and whose expression does not change in response to excess Zn^{2+} (Yamamoto and Ishihama, 2005).

3. Results and discussion

3.1. Nanoparticle characterisation

Commercially available, uncoated Z-Cote® zinc oxide nanoparticles were used in our experiments to demonstrate an *E. coli* 'whole cell biosensor assay' for ZnO dissolution and photo-radical generation in a complex medium. The ZnO nanoparticles have an irregular morphology and a mean diameter of 150 ± 60 nm in the Neidhardt's medium consistent with the size of the dry powder, Fig. 1A. This medium was chosen as it supports the growth of *E. coli* and suspensions of the nanoparticles were metastable over the time course of approximately 8 h, sufficient for microbiological experiments to be conducted. The stability of the ZnO nanoparticle suspensions was determined by measuring characteristic UV–vis absorption spectra of colloidal ZnO nanoparticles over time (data not shown). The size and shape of the nanoparticles, as well as

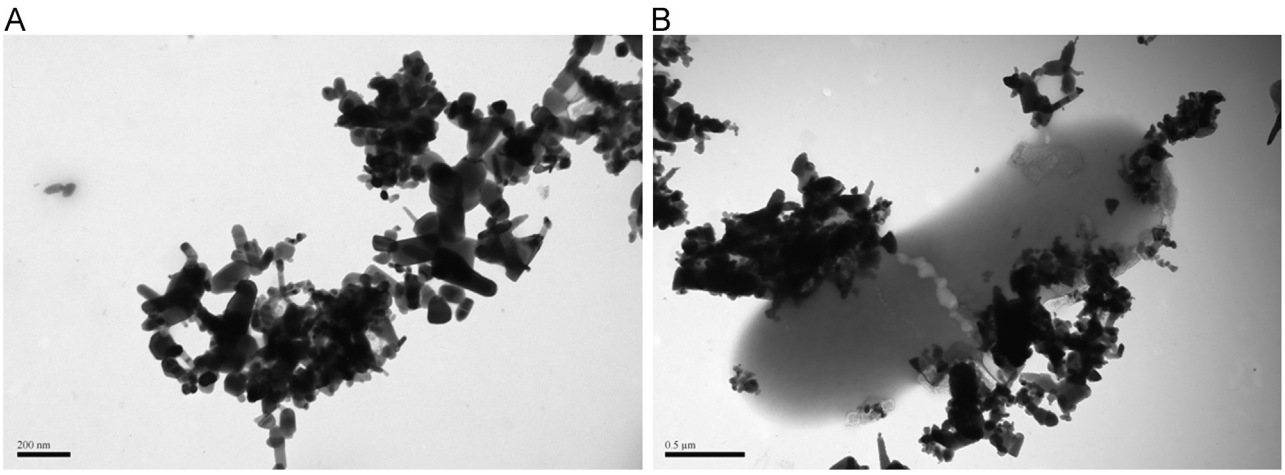

Fig. 1. Transmission Electron Micrographs showing the Z-Cote® ZnO nanoparticles suspended in the Neidhardt's medium (Panel A) and after suspension in the medium containing actively growing *E. coli* bacteria (Panel B). Typical images are shown.

their zeta potential determines their stability in suspension however zeta potential was not determined in this medium due to the high solution conductivity. Measured values for zeta potential in deionised water (24.3 ± 0.4 mV) and 5 mM NaCl (20.8 ± 0.8 mV) indicated a low stability consistent with nanoparticle aggregation seen in TEM images. The same aggregation can be observed in the presence of *E. coli*, wherein the ZnO nanoparticles form aggregates surrounding the cell surface, with the same caveat about the origin of the aggregation process, Fig. 1B.

3.2. Dissolution and photo-electron measurements and toxicity

ZnO dissolution in the Neidhardt's medium was measured by ultra-centrifugation to separate the nanoparticles from the medium followed by ICP-MS to measure total Zn in the supernatant. In a typical experiment the nanoparticles were suspended at a concentration of 100 μg mL^{-1} wherein the total Zn^{2+} rises from a background concentration of 0.137 ± 0.02 μg mL^{-1} to a maximum of 70.86 ± 0.85 μg mL^{-1} over 47 h, Fig. 2A. The rapid initial rate of dissolution may be attributed to incomplete separation of smaller nanoparticles from the medium and the asymptotic trend in dissolved Zn^{2+} concentration to the differential rate of dissolution in the nanoparticle size distribution with smaller nanoparticle dissolving more rapidly.

Zinc ions are toxic and nanoparticle dissolution in the minimal salts medium in the dark inhibits the growth of *E. coli* in a dose-dependent manner, Fig. 2B(i). Additionally, we compared the effects of Zn^{2+} with and without the nanoparticle present: *E. coli* were exposed to the nanoparticles or a concentration of Zn^{2+} (as $ZnCl_2$) equivalent to the measured concentration from nanoparticle dissolution. The inhibition of *E. coli* by the concentration of Zn^{2+} derived from the dissolution of the ZnO nanoparticles was greater than that by the same concentration of Zn^{2+} derived from the metal chloride, Fig. 2B(ii). As this experiment was carried out in the dark, this is not an additive effect from dual Zn^{2+}/ photo-electron toxicity. We attribute this effect to the nano-bio interface: Zn^{2+} is delivered proximal to the membrane creating a high interfacial concentration effect, whereas Zn^{2+} added as the chloride is quickly dispersed throughout the medium.

The UV–vis extinction of the ZnO nanoparticle suspensions in the Neidhardt's medium showed a single feature λ_{max} at approximately 375 nm, corresponding to the band-gap transition of ZnO. Generation of photo-electrons from the ZnO nanoparticles leading to DCPIP reduction is shown in Fig. 2C. The nanoparticle produces photo-electrons that reduce the DCPIP molecule (with a well-defined stoichiometry: one molecule requiring two electrons) causing a first-order exponential decay in the absorbance of the dye with a half-life of 37 min. The toxic effects of UV exposure with and without the ZnO nanoparticle photo-centre were measured in suspensions of the bacterium in water. A loss in *E. coli* viability was recorded between UV exposed and non-irradiated suspensions in water but the toxic effect was enhanced in the presence of the ZnO nanoparticles, Fig. 2D.

In the Neidhardt's medium the nanoparticle reduction of DCPIP was quenched, illustrating how it is difficult to measure this effect in a complex medium.

3.3. Whole cell bio-sensor assay

The whole cell bio-sensor approach was assessed as an alternative to the physical methods to measure simultaneously Zn^{2+} metal ion toxicity and photo-radical generation redox toxicity using transcriptional biomarkers for the corresponding toxic stress responses, Fig. 3A. The bacteria were exposed to the nanoparticles in the Neidhardt's medium, in the dark or with 375 nm UV light, and gene expression was compared with untreated controls.

ZnO nanoparticle dissolution was demonstrated by measuring transcriptional changes for genes encoding Zn^{2+} membrane transporters; *zntA* (Zn^{2+} efflux) and *znuABC* (Zn^{2+} import). The genes were inversely regulated in response to ZnO nanoparticles indicating nanoparticle dissolution leading to excess Zn^{2+} in the cytosol, Fig. 3B. The response is activated by external Zn^{2+} concentrations of at least 10 nM (0.65 μg/L) (Yamamoto and Ishihama, 2005), which confers greater sensitivity than optical emission methods but less sensitivity than mass spectrometry, which have limits of detection of approximately 5 μg/L and 0.01 μg/L respectively. In human tissues Zinc ion toxicity occurs typically at concentrations exceeding 60 ng/L (Nriagu, 2007), which is within the limit of detection for the whole cell bio-reporter. Furthermore, gene regulation is specific for Zn^{2+} (Outten et al., 1999; Patzer and Hantke, 2000) whereas ICP-MS only measures total Zn and the accuracy of the measurement depends on the removal of the nanoparticles by dialysis or ultra-centrifugation with size cut-off limitations.

Gene regulation is also shown for a $ZnCl_2$ control, where the bacteria were exposed to Zn^{2+} without the nanoparticles but in either case we used ICP-MS to determine that the solution phase Zn^{2+} concentration was equivalent (either added as $ZnCl_2$ or from nanoparticle dissolution). The regulation of Zn^{2+}-responsive genes was significantly enhanced (*T*-test, $P \leq 0.05$) for the nanoparticle, as was the toxic effect on bacterial growth shown in Fig. 2B(ii). The magnitude of the Zn^{2+}-induced transcription is proportional

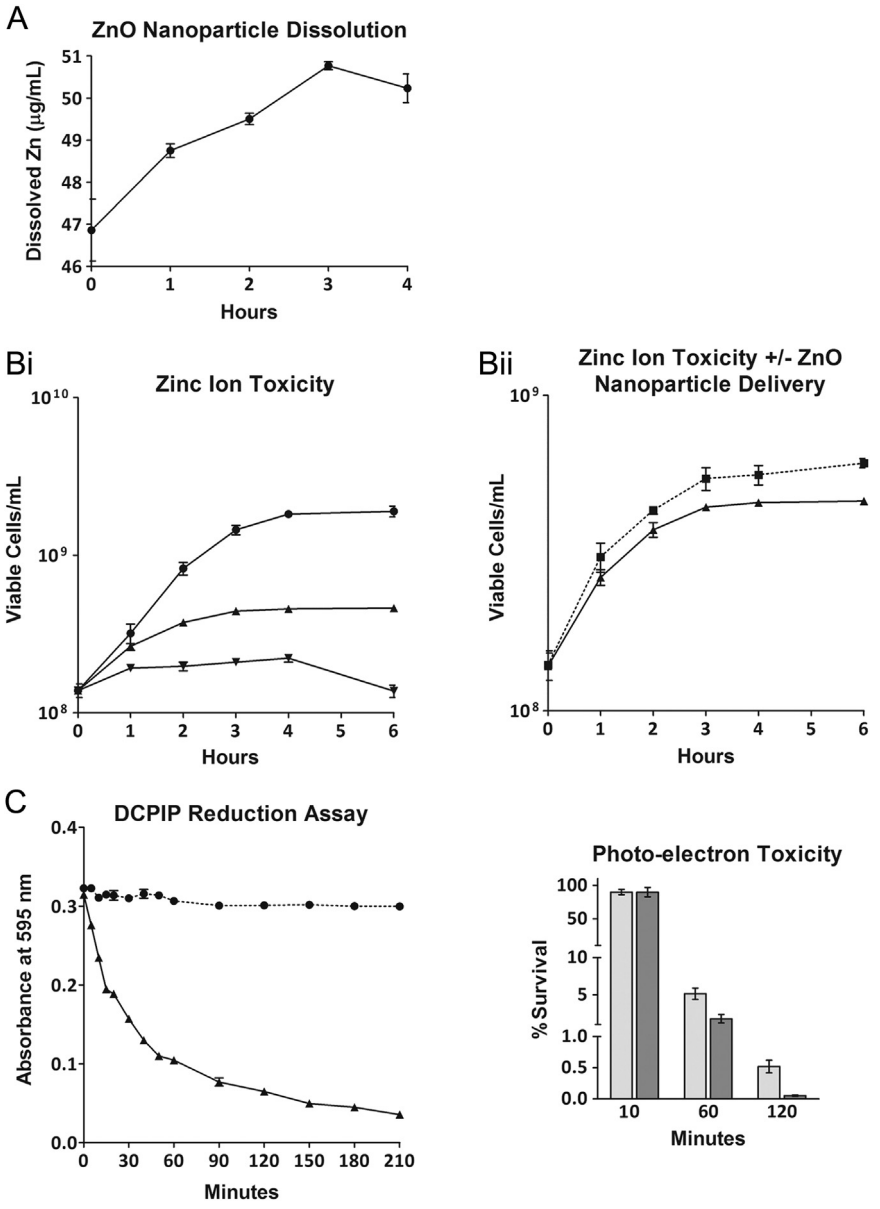

Fig. 2. Physical measurements of Z-Cote® ZnO nanoparticle dissolution and photo-electron production, leading to toxicity against *E. coli*. (A) The dissolution profile is shown for a suspension of 100 μg mL^{-1} of the nanoparticles in Neidhardt's minimal salts medium, and similar trends (not shown) were observed at higher concentrations. The measurements were made by ICP-MS after removing the nanoparticles by ultracentrifugation. The detection limit of this technique was 1.1 ng mL^{-1}, and the error bars show the a relative standard deviation from 5 replicate samples. (B)(i) The toxic effect of dissolution on *E. coli* growth in the medium: native growth curve (●), growth in a suspension of 100 μg mL^{-1} of the ZnO nanoparticles (▲) and growth in a suspension of 200 μg mL^{-1} of the ZnO nanoparticles (▼). Error bars are the standard error of the mean ($n=3$). (B)(ii) Growth curves for *E. coli* in medium containing ZnO nanoparticles (■) or zinc chloride added at the rate of nanoparticle dissolution (▲) allowing a comparison of the effects of Zn^{2+} with or without the nanoparticle present. Error bars are the standard error of the mean ($n=3$). (C) Photo-electron production leading to a colour change in the redox sensitive dye DCPIP. The dye was added to 100 μg mL^{-1} of the ZnO nanoparticles suspended in water, either in the dark (dotted line, ●) or in 375 nm light (solid line, ▲). Photo-electron production leads to reduction of the DCPIP molecule causing the change in absorbance at 595 nm. (D) Survival of *E. coli* in a suspension of 100 μg mL^{-1} of the ZnO nanoparticles in water, in the dark (light grey bars) or in 375 nm light (dark grey bars). Error bars are the standard error of the mean ($n=3$).

to the concentration of Zn^{2+} outside the cell (Yamamoto and Ishihama, 2005) and the specificity of the response for the zinc ion is evidence that this enhanced toxicity is the direct result of the interfacial Zn^{2+} concentration effect at the nano-bio interface and does not constitute an effect of the ZnO nanoparticle. A similar nanoparticle-enhanced toxicity has been reported by others (McQuillan et al., 2012; Navarro et al., 2008; Wang et al., 2009; Xiong et al., 2011).

We found that the DCPIP-based assay for photo-electron toxicity was incompatible with the complex medium which quenched the reduction of the DCPIP molecule. In contrast, a whole cell bio-reporter approach was not compromised in the same medium and transcriptional changes in response to photo-radical stress showed clearly that this process occurs and the resulting toxic stress response. The photo-radicals produced by the nanoparticles can directly or indirectly (through radical propagation) activate gene regulatory proteins SoxR and OxyR, leading to the expression of genes encoding SoxS and Catalase respectively, which are part of the *E. coli* response to oxidative stress, Fig. 3C. Both transcriptional biomarkers were also significantly increased (*T*-test, $P \leq 0.05$) between ZnO nanoparticle treated bacteria and untreated controls in the dark indicating that Zn^{2+} toxicity from nanoparticle dissolution also contributes to the oxidative stress response. However, there was a significant difference in the magnitude of the response between dark and UV irradiated samples showing clearly the photo-electron toxic response. The genes *sodA* and

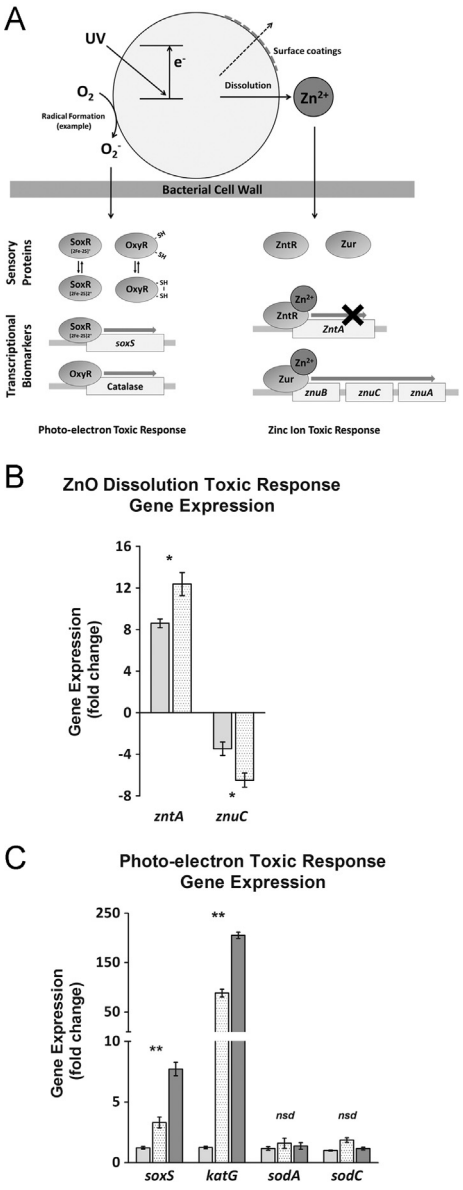

Fig. 3. A whole cell biosensor approach for simultaneous detection of dual ZnO nanoparticle toxicity mechanisms based on transcriptional biomarkers in *E. coli*. (A) A representation of the pathways leading to activation of transcriptional biomarkers for photo-electron (left side) and zinc ion (right side) toxic responses in *E. coli*. A ZnO nanoparticle in the extracellular medium or attached to the membrane delivers photo-electrons (leading to the generation of free radicals) under UV light, and simultaneously dissolves to release Zn^{2+}. Free radicals and Zn^{2+} in the metabolism of the bacterium interact with gene regulatory proteins leading to a change in the expression of genes to counteract the toxic species. (B) Regulation of Zn^{2+}-responsive genes was measured in the Neidhardt's medium after exposure for 10 minutes to Zn^{2+} as zinc chloride (light grey bars) or 100 μg mL^{-1} of the ZnO nanoparticles (white shaded bars). The concentration of $ZnCl_2$ was adjusted to the measured bulk solution phase Zn from the nanoparticles dissolving. Asterisks indicate statistically significant differences (*T*-test, $P \leq 0.05$). The reported values are relative to untreated controls. The error bars are the standard error of the mean ($n=3$). (C) Regulation of free radical-responsive genes was measured in the Neidhardt's medium after exposure for 10 min to UV light (light grey bars), or to 100 μg mL^{-1} of the ZnO nanoparticles in the dark (white shaded bars), or to UV light and nanoparticles simultaneously (dark grey bars). Double asterisks indicate statistically significant differences between the different exposures (*T*-test, $P \leq 0.05$), or no significant differences (nsd). The reported values are relative to untreated controls. The error bars are the standard error of the mean ($n=3$).

sodC surprisingly did not show any significant regulation following exposure to the nanoparticles, either in the dark or under UV light. The *sodA* gene is positively regulated by SoxS, however another level of regulation for this gene must exist such that it was not transcribed even though *soxS* was expressed at high levels. In contrast the *sodC* gene is regulated by the *rpoS* sigma factor, associated with stationary phase and its response may be limited to this growth phase whereas experiments were always conducted using bacteria harvested during log phase.

4. Conclusions

In conclusion, we have demonstrated that a dispersion of Z-Cote ZnO nanoparticles has two toxicity mechanisms; Zn^{2+} toxicity following nanoparticle dissolution and free radical toxicity following photo-electron production in ultraviolet light. Dissolution measured by ultra-centrifugation (or other techniques such as dialysis) followed by total Zn determination by ICP-MS can give results that depend on the low-mass cut-off efficiency of the nanoparticle separation process. Detection of photo-electron production in a complex medium using a redox dye is hindered by competing radical capture reactions. The whole cell bio-sensor quantitative gene expression assay, however, is a direct simultaneous measure of both toxicity mechanisms in a complex medium. Zinc ion stress and photo-radical stress transcriptional response profiles can discriminate between the Zn^{2+} dissolution product and whole ZnO nanoparticles producing photo-electrons to detect zinc speciation.

Acknowledgements

J. McQuillan would like to thank the BBSRC for a CASE award with ENBL Ltd.

Appendix A. Supporting Information

Supplementary data associated with this article can be found in the online version at http://dx.doi.org/10.1016/j.bios.2013.07.024.

References

Beard, S.J., Hashim, R., Membrillo-Hernandez, J., Hughes, M.N., Poole, R.K., 1997. Molecular Microbiology 25 (5), 883–891.
Binet, M.R., Poole, R.K., 2000. FEBS Letters 473 (1), 67–70.
Bousse, L., 1996. Sensors and Actuators B: Chemical 34 (1–3), 270–275.
Brocklehurst, K.R., Hobman, J.L., Lawley, B., Blank, L., Marshall, S.J., Brown, N.L., Morby, A.P., 1999. Molecular Microbiology 31 (3), 893–902.
Comparelli, R., Fanizza, E., Curri, M.L., Cozzoli, P.D., Mascolo, G., Agostiano, A., 2005. Applied Catalysis B: Environmental 60 (1–2), 1–11.
Demple, B., 1999. Clinical and Experimental Pharmacology and Physiology 26 (1), 64–68.
Gulson, B., McCall, M., Korsch, M., Gomez, L., Casey, P., Oytam, Y., Taylor, A., Kinsley, L., Greenoak, G., 2010. Toxicological Sciences 120 (2), 140–149.
Hoffmann, M.R., Martin, S.T., Choi, W., Bahnemann, D.W., 1995. Chemical Reviews 95 (1), 69–96.
Ivask, A., Bondarenko, O., Jepihhina, N., Kahru, A., 2010. Analytical and Bioanalytical Chemistry 398 (2), 701–716.
Ivask, A., Rolova, T., Kahru, A., 2009. BMC Biotechnology 9, 41.
Ivask, A., Virta, M., Kahru, A., 2002. Soil Biology and Biochemistry 34 (10), 1439–1447.
Keseler, I.M., Collado-Vides, J., Santos-Zavaleta, A., Peralta-Gil, M., Gama-Castro, S., Muniz-Rascado, L., Bonavides-Martinez, C., Paley, S., Krummenacker, M., Altman, T., Kaipa, P., Spaulding, A., Pacheco, J., Latendresse, M., Fulcher, C., Sarker, M., Shearer, A.G., Mackie, A., Paulsen, I., Gunsalus, R.P., Karp, P.D., 2011. Nucleic Acids Research 39(Database Issue), D583–590.
Klingshirn, C., 2007. ChemPhysChem 8 (6), 782–803.
McQuillan, J.S., Infante, H.G., Stokes, E., Shaw, A.M., 2012. Nanotoxicology 6, 857–866.
Miao, A.J., Zhang, X.Y., Luo, Z., Chen, C.S., Chin, W.C., Santschi, P.H., Quigg, A., 2010. Environmental Toxicology and Chemistry/SETAC 29 (12), 2814–2822.
Mills, A., Le Hunte, S., 1997. Journal of Photochemistry and Photobiology A: Chemistry 108 (1), 1–35.

Mitchell, R.J., Gu, M.B., 2004. Applied Microbiology and Biotechnology 64 (1), 46–52.
Mitchnick, M.A., Fairhurst, D., Pinnell, S.R., 1999. Journal of the American Academy of Dermatology 40 (1), 85–90.
Navarro, E., Piccapietra, F., Wagner, B., Marconi, F., Kaegi, R., Odzak, N., Sigg, L., Behra, R., 2008. Environmental Science and Technology 42 (23), 8959–8964.
Neidhardt, F.C., Bloch, P.L., Smith, D.F., 1974. Journal of Bacteriology 119 (3), 736–747.
Nriagu, J., 2007. Zinc Toxicity in Humans. School of Public Health, University of Michigan.
Outten, C.E., O'Halloran, T.V., 2001. Science 292 (5526), 2488–2492.
Outten, C.E., Outten, F.W., O'Halloran, T.V., 1999. Journal of Biological Chemistry 274 (53), 37517–37524.
Patzer, S.I., Hantke, K., 1998. Molecular Microbiology 28 (6), 1199–1210.
Patzer, S.I., Hantke, K., 2000. Journal of Biological Chemistry 275 (32), 24321–24332.
Pfaffl, M.W., 2001. Nucleic Acids Research 29 (9), e45.
Rensing, C., Mitra, B., Rosen, B.P., 1997. Proceedings of the National Academy of Sciences of the United States of America 94 (26), 14326–14331.
Riether, K.B., Dollard, M.A., Billard, P., 2001. Applied Microbiology and Biotechnology 57 (5–6), 712–716.
Waalewijn-Kool, P.L., Diez Ortiz, M., van Straalen, N.M., van Gestel, C.A.M., 2013. Environmental Pollution 178 (0), 59–64.
Wang, H., Wick, R.L., Xing, B., 2009. Environmental Pollution 157 (4), 1171–1177.
Xiong, D., Fang, T., Yu, L., Sima, X., Zhu, W., 2011. Science of the Total Environment 409 (8), 1444–1452.
Yamamoto, K., Ishihama, A., 2005. Journal of Bacteriology 187 (18), 6333–6340.